Molecular Therapy
Nucleic Acids
Original Article

# MicroRNA-4500 Inhibits Migration, Invasion, and Angiogenesis of Breast Cancer Cells via RRM2-Dependent MAPK Signaling Pathway

Shaoying Li,[1] Huifen Mai,[2] Yefeng Zhu,[1] Guofeng Li,[3] Jing Sun,[2] Guisen Li,[1] Bichan Liang,[1] and Shaojun Chen[4]

[1]Department of Thyroid and Breast Surgery, Shenzhen Baoan Women's and Children's Hospital, Jinan University, Sanming Project of Medicine in Shenzhen, Shenzhen 518000, P.R. China; [2]Department of Gynaecology, Shenzhen Baoan Women's and Children's Hospital, Jinan University, Shenzhen 518000, P.R. China; [3]Department of Chest Surgery, Shenzhen People's Hospital, Shenzhen 518000, P.R. China; [4]Department of Breast Surgery, Shenzhen Maternity and Child Health Hospital, Shenzhen 518000, P.R. China

**With the consideration of the dynamic role of microRNAs (miRNAs) in breast cancer, miRNAs may serve as therapeutic targets, helping to prevent development of therapy resistance, maintain stable disease, and prohibit metastatic spread. We identified the differentially expressed breast cancer-related gene ribonucleotide reductase subunit M2 (RRM2) as the study focus through microarray expression profiles. Next, the upstream regulatory microRNA (miR)-4500 of RRM2 was predicted using bioinformatics website analysis, and their binding was verified by a dual luciferase reporter gene assay. The regulatory effects of miR-4500 on breast cancer cell proliferation, apoptosis, migration, invasion, and capillary-like tube formation of endothelial cells were assessed by gain- and loss-of-function experiments. The experimental data revealed that miR-4500 was downregulated, whereas RRM2 was upregulated in breast cancer cells. Mechanistic analysis revealed that miR-4500 downregulated the RRM2 expression to inactivate the mitogen-activated protein kinase (MAPK) signaling pathway. Furthermore, miR-4500 exerted anti-tumor effects by targeting RRM2 through suppression of the MAPK signaling pathway *in vitro*, evidenced by attenuated cancer cell migration and invasion and capillary-like tube formation of endothelial cells. The *in vivo* experiments further corroborated *in vitro* results. Collectively, overexpressed miR-4500 could downregulate RRM2 and inhibit activation of the MAPK signaling pathway, thus attenuating breast cancer cell proliferation, invasion, migration, and angiogenesis and promoting breast cancer cell apoptosis.**

## INTRODUCTION

Breast cancer, a predominant, common tumor among females worldwide, is the main cause of cancer-related deaths in women, accounting for 10% of the new malignancies diagnosed every year across the world and 22% of malignancies among females.[1] Over the past decade, the incidence rate of breast cancer has been on the rise across the world, including China, a country with historically lower incidence rates of the malignancy.[2] Numerous factors have been elucidated to greatly influence the fate of breast cancer, such as increasing age, reproductive factors, mammographic density, and genetic factors.[3] One of the most useful therapeutic strategies for breast cancer is chemotherapy, but the effects are limited due to the emergence of drug resistance and adverse effects of anti-tumor drugs.[4] Interestingly, abundant profiles have indicated that microRNAs (miRNAs) play a significant role in tumor proliferation, progression, and metastasis through the regulation of genes.[5]

miRNAs are defined as small noncoding RNAs of 18–24 nt, which possess the ability to modulate gene expression through binding to the 3′ untranslational region (3′ UTR) of target messenger RNAs (mRNAs), and genetic variants in miRNA target sites have been widely correlated with human diseases.[6] One such miRNA, miR-4500, is known to exert a suppressive effect on the growth of tumor cells, whereas downregulation of miR-4500 has been shown to promote growth of non-small cell lung cancer (NSCLC).[7] Moreover, it is revealed that miR-4500 is capable of suppressing cell proliferation, migration, and invasion and tumor growth in colorectal cancer (CRC).[8] The bioinformatics website http://www.targetscan.org/vert_71/ and dual luciferase reporter gene assay in the current study have suggested that ribonucleotide reductase subunit M2 (RRM2) is the target gene of miR-4500. RRM2 is encoded by different genes on separate chromosomes, of which its mRNA is differentially expressed throughout the cell cycle.[9] In addition, existing evidence also suggests that the p38 mitogen-activated protein kinase (MAPK) signaling pathway participates in cell proliferation, differentiation, and migration of breast cancer.[10] Therefore, it is implied that miR-4500 might influence breast cancer development, which may implicate RRM2 and the MAPK signaling pathway; thus, the current study aims to shed new light on the relationship of miR-4500, RRM2, and the MAPK signaling pathway in the regulation of breast cancer cells.

Received 19 February 2020; accepted 29 April 2020;
https://doi.org/10.1016/j.omtn.2020.04.018.

**Correspondence:** Shaoying Li, Shenzhen Baoan Women's and Children's Hospital, Jinan University, Sanming Project of Medicine in Shenzhen, No. 56, Yulv Road, Baoan District, Shenzhen 518000, Guangdong Province, P.R. China.
**E-mail:** lsy_lishaoying@163.com

 

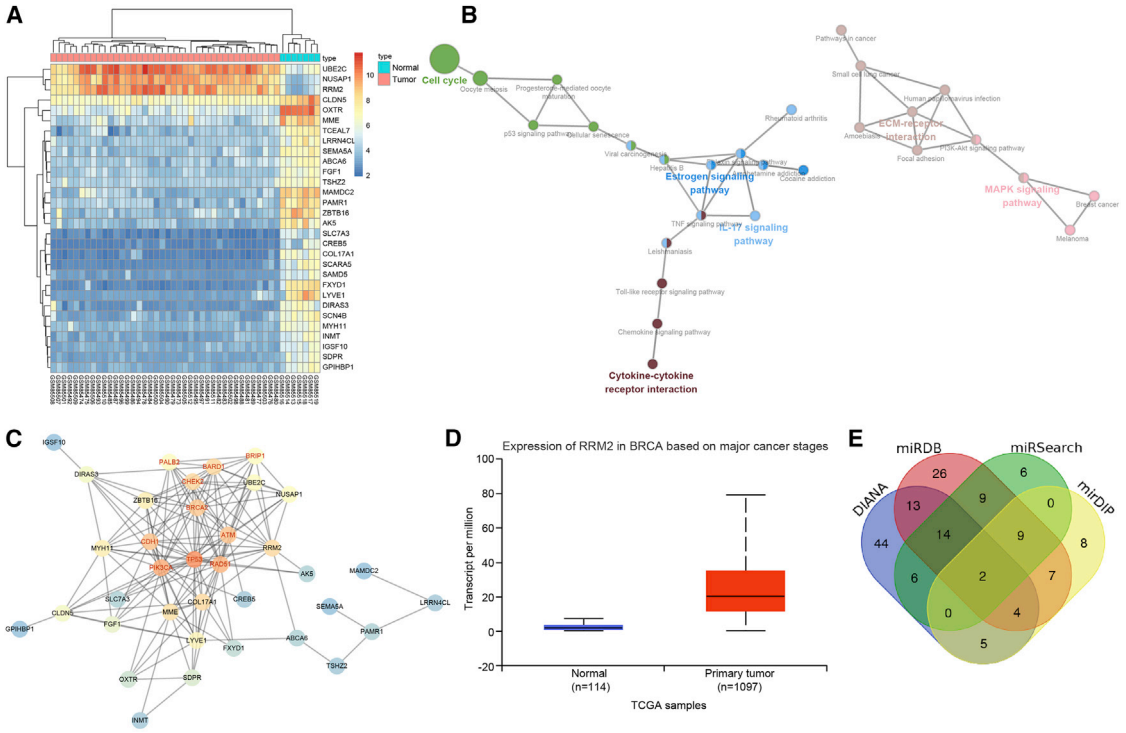


**Figure 1. miR-4500 Influences the Development of Breast Cancer through Regulation of the RRM2-Dependent MAPK Signaling Pathway**

(A) The heatmap of variance analysis in breast cancer expression microarray data, wherein the abscissa represents the sample number, the ordinate represents the gene name, the upper dendrogram shows the sample-type clustering analysis, the ordinate represents the gene-expression level clustering, and each small square in the figure represents the expression level of a gene in a sample. (B) KEGG analysis of DEGs in breast cancer expression microarray data, wherein each circle represents a name of a disease or a name of KEGG entry, and the lines between the circles indicate their relationship. (C) The interaction network graph between known genes and DEGs in breast cancer, wherein each circle represents a gene, and the lines between the two circles indicate the interaction between the two genes. The red font represents the known genes related to breast cancer retrieved from the database. The circle color indicates the core degree of the gene in the network graph. The darker color reflects the higher core degree. (D) The expression analysis of the RRM2 gene in TCGA breast cancer database; the abscissa indicates the sample type, the ordinate indicates the gene-expression level, the left box shows the expression of RRM2 in normal samples, and the right box shows the expression of RRM2 in breast cancer samples. (E) The prediction results of regulatory miRNAs toward RRM2. The four ellipses in the figure represent the prediction results of four databases, and the middle part represents the intersection of them; besides, the numbers in the figure represent the number of miRNAs in each area.

## RESULTS

### Bioinformatics Analysis to Predict the Differentially Expressed Genes (DEGs) and Their Molecular Interactions in Breast Cancer

The Gene Expression Omnibus (GEO) database was utilized to retrieve the microarray data GEO: GSE3744. DEGs in the breast cancer samples and normal samples of GEO: GSE3744 were analyzed, and finally, 442 DEGs were obtained. Among the obtained genes, 133 were significantly upregulated in breast cancer samples, whereas 309 were notably downregulated. Figure 1A depicts a heatmap of the top 30 DEGs in GEO: GSE3744. Further, Kyoto Encyclopedia of Genes and Genomes (KEGG) analysis was employed to analyze the DEGs in GEO: GSE3744 (Figure 1B), which revealed that these DEGs were enriched in the cell cycle and the MAPK signaling pathway. In addition, enrichment analysis results indicated that the MAPK signaling pathway was closely related to breast cancer. The KEGG database was further adopted to retrieve breast cancer-related signaling pathways, and the MAPK signaling pathway played an important role in breast cancer (map05224). The MalaCards database was further retrieved to search for known breast cancer-related genes (Table 1). Then, correlation analysis was performed between the known genes obtained from the MalaCards database and the DEGs in breast cancer obtained by microarray-based gene-expression analysis, and a gene-interaction network was constructed subsequently (Figure 1C). The results demonstrated that RRM2 and COL17A1 were at the core position of all the DEGs, and RRM2 presented with direct or indirect interactions with 9 of the known breast cancer genes. Moreover, RRM2 exhibited a greater differential multiple in GEO: GSE3744 compared to COL17A1. Consequently, RRM2 was selected as the focus for follow-up experimentation. Furthermore, the expression of RRM2 for breast cancer was retrieved from The Cancer Genome Atlas (TCGA) database (Figure 1D), which illustrated that RRM2 was also highly expressed in breast cancer. Moreover, several studies have indicated that RRM2 is closely related with the MAPK signaling pathway.[11,12] All of the analysis results and previous reports suggested that RRM2 was most likely to function in breast cancer through the MAPK signaling pathway. Additionally, the regulatory miRNAs toward RRM2 were predicted

**Table 1. The Known Breast Cancer-Related Genes (Top 10)**

| Symbol | Description | Score | PubMed IDs |
|---|---|---|---|
| BRCA2 | BRCA2, DNA repair associated | 1,422.74 | 20301425, 15604628, 18163131 |
| CHEK2 | checkpoint kinase 2 | 1,366.3 | 20301425, 15604628, 18163131 |
| RAD51 | RAD51 recombinase | 1,320.91 | 10807537, 20301425, 15604628 |
| PIK3CA | phosphatidylinositol-4,5-bisphosphate 3-kinase catalytic subunit alpha | 1,300.3 | 17954709, 23917950, 23970019 |
| BRIP1 | BRCA1-interacting protein C-terminal helicase 1 | 1,253.24 | 11301010, 17954709, 23917950 |
| CDH1 | cadherin 1 | 1,166.03 | 17660459, 17954709, 23917950 |
| PALB2 | partner and localizer of BRCA2 | 1,047.25 | 20301425, 15604628, 18163131 |
| ATM | ATM serine/threonine kinase | 1,037.36 | 10571946, 20301425, 15604628 |
| BARD1 | BRCA1-associated ring domain 1 | 1,021.62 | 20301425, 15604628, 18163131 |
| TP53 | tumor protein P53 | 996.4 | 20301425, 15604628, 18163131 |

Symbol represents the abbreviation of genes; description represents details or full name of genes; score originates from Solr-based GeneCards search-engine score, obtained by querying the disease in GeneCards; PubMed identifications (IDs) represent the reference number PubMed identifier (PMID) of the gene related to breast cancer. ATM, ataxia telangiectasia mutated.

(Figure 1E), and the intersection was adopted, which yielded two regulatory miRNAs: miR-4500 and miR-98. The influence of miR-98 on breast cancer and its related mechanisms in a variety of tumors has already been well studied,[13–16] whereas miR-4500 has been rarely reported in tumors, and the related research in breast cancer is much scarcer. All of these results suggested that miR-4500 might regulate the MAPK signaling pathway through regulation of RRM2 to affect the development of breast cancer.

### miR-4500 Is Poorly Expressed in Breast Cancer Cells

Next, quantitative reverse transcriptase polymerase chain reaction (qRT-PCR) was applied to determine the expression of miR-4500 in MCF7, BT474, MDA-MB-468, MDA-MB-231, and MCF10A cell lines (Figure 2). miR-4500 was poorly expressed in MCF7, BT474, MDA-MB-468, and MDA-MB-231 cells compared with that in MCF10A cells. More specifically, MCF7 cells exhibited the lowest miR-4500 expression among all of the cell lines ($p < 0.05$). Therefore, the breast cancer cell line MCF7 was selected for subsequent experimentation.

### miR-4500 Targets and Downregulates RRM2

Bioinformatics website (http://www.targetscan.org/vert_71/) and dual luciferase reporter gene assay predicted that miR-4500 targeted RRM2 and the presence of a specific binding region between the RRM2 gene sequence and miR-4500 sequence (Figure 3A). Subsequently, a dual luciferase reporter gene assay was employed to verify

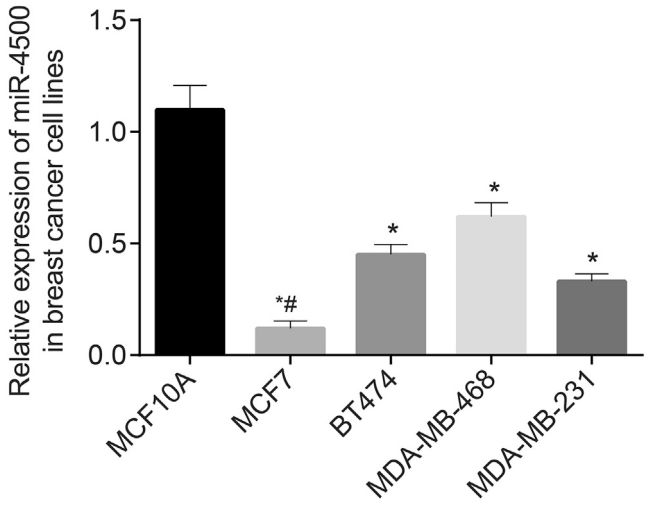


**Figure 2. miR-4500 Is Poorly Expressed in Breast Cancer Cell Lines**

*$p < 0.05$ versus normal breast epithelial cell line MCF10A; #$p < 0.01$ versus breast cancer cell line MCF7. Data were analyzed by one-way ANOVA, and the experiment was repeated three times independently.

whether RRM2 was the target gene of miR-4500. The results (Figure 3B) showed that the luciferase activity of wild-type (WT)-miR-4500/RRM2 in the miR-4500 mimic group was declined compared with that in the mimic negative control (NC) group ($p < 0.05$), whereas there were no significant differences in the luciferase activity of mutant type (MUT)-miR-4500/RRM2 ($p > 0.05$), which verified that miR-4500 could specifically bind to the RRM2 gene.

Additionally, qRT-PCR and western blot analysis were adopted in order to detect the expression of miR-4500 and RRM2 in transfected cells. The results (Figures 3C–3E) demonstrated that the miR-4500 mimic group presented with significantly increased miR-4500 levels and markedly decreased RRM2 levels compared to the mimic NC group ($p < 0.05$). In contrast to the small interfering RNA (siRNA) targeting NC (si-NC) group, there were no significant changes in the expression of miR-4500 ($p > 0.05$), whereas RRM2 expression was decreased in the si-RRM2 group ($p < 0.05$). Compared with the miR-4500 inhibitor group, the expression of miR-4500 did not differ significantly ($p > 0.05$), whereas the expressions of RRM2 mRNA and protein were obviously reduced ($p < 0.05$) in the miR-4500 inhibitor + si-RRM2 group. All of these results showed that overexpression (oe) of miR-4500 downregulated RRM2.

### Overexpression of miR-4500 Downregulates RRM2 to Inhibit Breast Cancer Cell Proliferation

After the elucidation that miR-4500 downregulated RRM2, the 5-ethynyl-2′-deoxyuridine (EdU) proliferation assay and western blot analysis were adopted in order to detect the EdU-positive cells and the expression of proliferation-related factors Ki67 and proliferating cell nuclear antigen (PCNA) (Figures 4A–4D). Compared with the mimic NC group, the EdU-positive expression rate was obviously reduced, and the expression of RRM2, Ki67, and PCNA decreased in

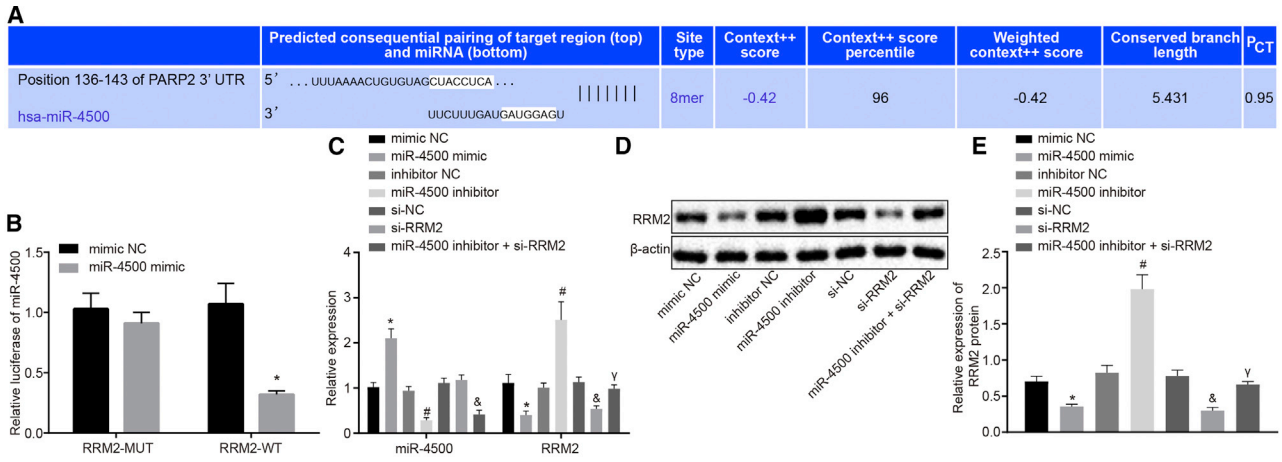


**Figure 3. RRM2 Is a Target Gene of miR-4500**

(A) The predicted binding sites of miR-4500 and RRM2 3′ UTR. (B) The dual luciferase reporter gene assay for detecting luciferase activity. (C) The expressions of miR-4500 and RRM2 detected by qRT-PCR. (D) The electrophoresis strip of RRM2 protein detected by western blot analysis. (E) The expressions of RRM2 protein detected by western blot analysis. *, #, &, and γp < 0.05 versus the mimic NC group, inhibitor NC group, si-NC group, and miR-4500 inhibitor group, respectively. (B) The data comparison was analyzed by unpaired t test, and (C and E) the data were analyzed by one-way ANOVA. The experiment was repeated three times independently.

the miR-4500 mimic group (all $p < 0.05$), indicating that breast cancer cell proliferation was attenuated. Compared with the si-NC group, the EdU-positive expression rate was significantly reduced, whereas the expression of RRM2, Ki67, and PCNA was decreased in the si-RRM2 group (all $p < 0.05$), also suggesting that proliferation was inhibited. Compared with the si-RRM2 group, the EdU-positive expression rate and the proliferative ability of cells were markedly enhanced in the miR-4500 inhibitor + si-RRM2 group ($p < 0.05$).

Then, both RRM2 and miR-4500 were overexpressed in breast cancer cells, followed by quantification of miR-4500 expression. No significant differences were noted regarding the miR-4500

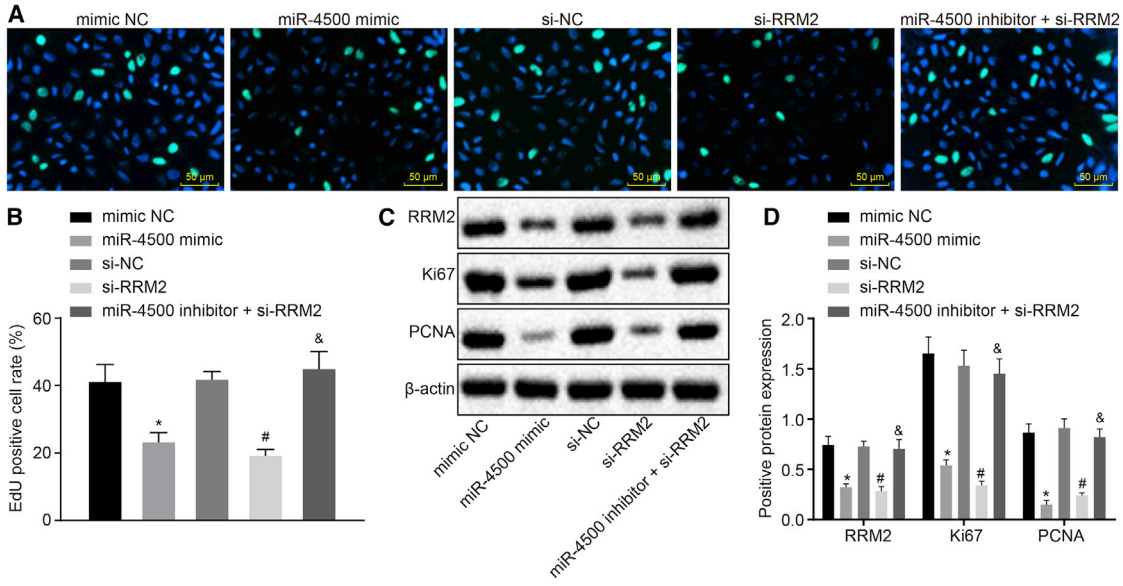


**Figure 4. Overexpression of miR-4500 Represses the Expression of RRM2 to Inhibit Breast Cancer Cell Proliferation**

(A) The cell proliferation detected by the EdU proliferation assay (400×). (B) Quantitative analysis for EdU-positive breast cancer cells detected by the EdU proliferation assay. (C) The protein protein expressions of RRM2 and cell proliferation-related factors Ki67 and PCNA detected by Western blot. (D) Comparison of relative protein expressions of RRM2 and cell proliferation-related factors Ki67 and PCNA in each group.. The data comparisons were analyzed by one-way ANOVA, and the experiment was repeated three times independently.

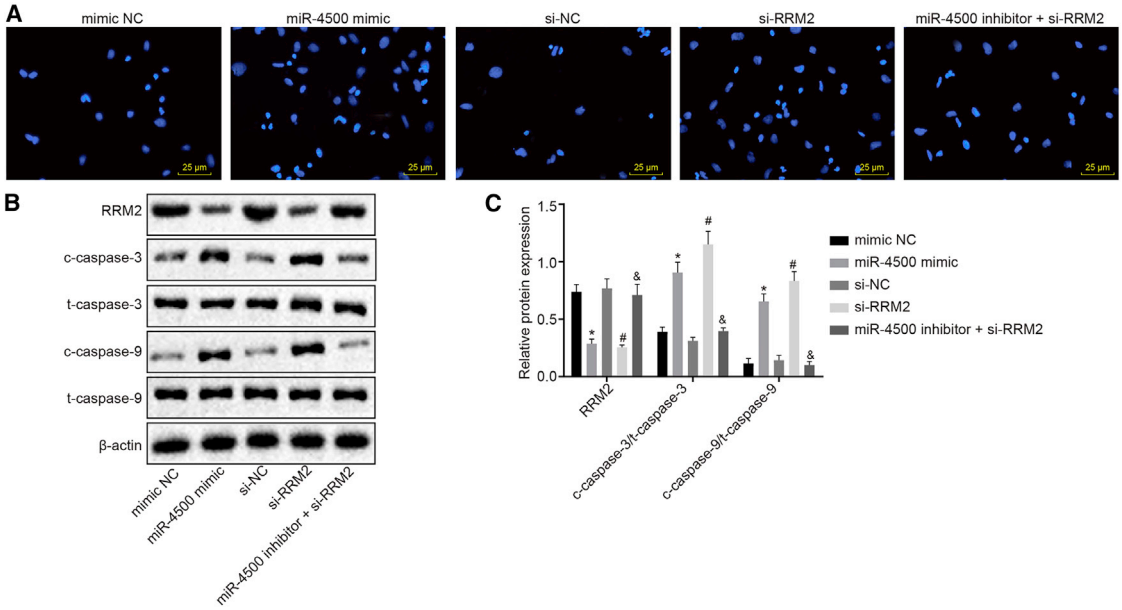


**Figure 5. Overexpression of miR-4500 Inhibits the Expression of RRM2 to Promote Breast Cancer Cell Apoptosis**

(A) The cell apoptosis detected by Hoechst staining (400×). (B) The protein bands of cell apoptosis-related factors c-caspase-3/t-caspase-3 and c-caspase-9/t-caspase-9 detected by western blot analysis. (C) The protein-expression patterns of cell apoptosis-related factors c-caspase-3/t-caspase-3 and c-caspase-9/t-caspase-9 in each group detected by western blot analysis. *, #, and &p < 0.05 versus the mimic NC group, si-NC group, and si-RRM2 group, respectively. The data comparisons were analyzed by one-way ANOVA, and the experiment was repeated three times independently.

expression between the oe-NC and oe-RRM2 groups ($p > 0.05$), whereas significantly high miR-4500 expression was observed in the miR-4500 mimic + oe-RRM2 group compared to the oe-RRM2 group ($p < 0.05$) (Figure S1A). In addition, results of the EdU assay and western blot analysis for cell-proliferation assessment showed that the EdU-positive expression rate was significantly elevated in the oe-RRM2 group in comparison to the oe-NC group, along with increased expressions of RRM2, Ki67, and PCNA. Meanwhile, opposite trends were detected in the miR-4500 mimic + RRM2 group compared to the oe-RRM2 group ($p < 0.05$) (Figures S1B–S1E). All of these results illustrated that overexpression of miR-4500 inhibited breast cancer cell proliferation by downregulation of RRM2.

### Overexpression of miR-4500 Downregulates RRM2 to Promote Breast Cancer Cell Apoptosis

Hoechst staining and western blot analysis were employed to detect the intensity of blue fluorescent staining of cells and the expression of apoptosis-related factors in breast cancer cells (Figures 5A–5C). Compared with the mimic NC group, the intensity of blue fluorescent staining of cells was increased, and the expression of cleaved-caspase-3/total-caspase-3 (c-caspase-3/t-caspase-3) and cleaved-caspase-9/total-caspase-9 (c-caspase-9/t-caspase-9) was significantly increased in the miR-4500 mimic group, in addition to reduced levels of RRM2 (all $p < 0.05$). In comparison with the si-NC group, the si-RRM2 group yielded results of similar changing tendency (all $p < 0.05$). Compared with the si-RRM2 group, the apoptosis rate of breast cancer cells in the miR-4500 inhibitor + si-RRM2 group was significantly reduced ($p < 0.05$).

Subsequently, combined overexpression of RRM2 and miR-4500 was induced in breast cancer cells, followed by Hoechst staining assay and western blot analysis to evaluate cell apoptosis (Figure S2). In comparison with the oe-NC group, fewer blue-stained cells were observed in the oe-RRM2 group, along with diminished levels of c-caspase-3/p-caspase-3 and c-caspase-9/t-caspase-9 ($p < 0.05$). Opposite trends were witnessed in the miR-4500 mimic + oe-RRM2 group when compared with the oe-RRM2 group ($p < 0.05$), all of which suggested that overexpression of miR-4500 promoted breast cancer cell apoptosis through downregulation of RRM2.

### Overexpression of miR-4500 Downregulates RRM2 to Inhibit Breast Cancer Cell Migration and Invasion

Transwell assay and western blot analysis were utilized to investigate the migration and invasion abilities of breast cancer cells (Figures 6A–6E). Compared with the mimic NC group, the expression of RRM2 and migration and invasion-related factors matrix metalloproteinase (MMP)-2 and MMP-9 was significantly decreased in the miR-4500 mimic group, which was highly suggestive of weakened cell migration and invasion (all $p < 0.05$). In contrast to the si-NC group, the expression of RRM2, MMP-2, and MMP-9 in the si-RRM2 group was all obviously decreased in the miR-4500 mimic group (all $p < 0.05$), indicating that the migration and invasion abilities were markedly suppressed. Compared with the si-RRM2 group, the migration and

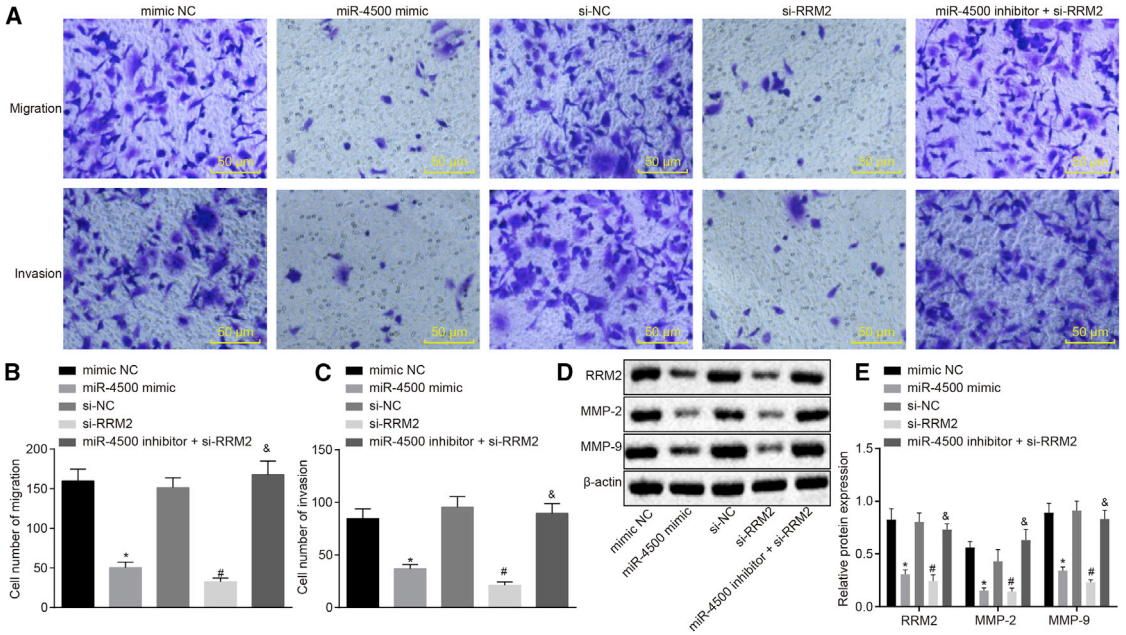


**Figure 6. Overexpression of miR-4500 Suppresses the Expression of RRM2 to Inhibit Breast Cancer Cell Migration and Invasion**

(A) The migration and invasion of breast cancer cells in each group under the microscope (200×). (B) The cell migration in each group detected by Transwell assay. (C) The cell invasion in each group detected by Transwell assay. (D) The protein expressions of RRM2, MMP-2 and MMP-9 detected by Western blot. (E) Comparison of relative protein expressions of RRM2, MMP-2 and MMP-9 in each group. The data comparisons were analyzed by one-way ANOVA, and the experiment was repeated three times independently.

invasion abilities of cells were significantly promoted in the miR-4500 inhibitor + si-RRM2 group ($p < 0.05$).

Next, breast cancer cells were treated with oe-RRM2 and miR-4500 mimic, and cell-migration and -invasion abilities were assessed using Transwell assay and western blot analysis (Figure S3). Compared with the oe-NC group, cell-migration and -invasion abilities were enhanced in the oe-RRM2 group, as indicated by significantly increased levels of MMP-2 and MMP-9, whereas the miR-4500 mimic + oe-RRM2 group exhibited opposite changing tendency in comparison to the oe-RRM2 group ($p < 0.05$). These findings demonstrated that miR-4500 downregulated RRM2 to suppress migration and invasion of breast cancer cells.

### Overexpression of miR-4500 Inhibits Angiogenesis of Breast Cancer Cells through Downregulation of RRM2

The capillary-like tube formation of endothelial cells *in vitro*, as well as western blot analysis for quantification of tumor angiogenic factors tissue inhibitor of metalloproteinases 2 (TIMP-2), vascular endothelial growth factor (VEGF), and vascular endothelial (VE)-cadherin, was applied (Figures 7A–7D). Compared with the mimic NC group, the number of capillary-like tubes of endothelial cells in the miR-4500 mimic group was significantly reduced, and the expressions of RRM2, TIMP-2, VEGF, and VE-cadherin significantly decreased (all $p < 0.05$). Relative to the si-NC group, the number of capillary-like tubes of endothelial cells was significantly reduced, and the expressions of RRM2, TIMP-2, VEGF, and VE-cadherin were significantly decreased in the si-RRM2 group (all $p < 0.05$). Compared with the si-RRM2 group, the number of capillary-like tubes of endothelial cells and the expressions of RRM2, TIMP-2, VEGF, and VE-cadherin were all significantly increased in the miR-4500 inhibitor + si-RRM2 group (all $p < 0.05$).

RRM2 and miR-4500 were then overexpressed in breast cancer cells, followed by an *in vitro* capillary-like tube-formation assay, as well as western blot analysis. As shown in Figure S4, more capillary-like tubes were observed in the oe-RRM2 group, along with significantly higher VEGF expressions, compared to those in the oe-NC group, whereas fewer capillary-like tubes were observed in the miR-4500 mimic + oe-RRM2 group, along with significantly lower VEGF expressions than those in the oe-RRM2 group ($p < 0.05$). These results indicated that miR-4500 downregulated RRM2 to inhibit capillary-like tube formation of endothelial cells, corresponding to suppressed angiogenesis in breast cancer cells.

### Overexpression of miR-4500 Downregulates RRM2 to Inhibit the Activation of the MAPK Signaling Pathway

Western blot analysis was adopted to detect the expressions of MAPK signaling pathway-related factors in order to further explore the effects of the downstream pathway. The results (Figures 8A and 8B) demonstrated that in comparison to the mimic NC group, the expressions of phosphorylated extracellular-regulated kinase 1/2 (p-ERK1/2)/total (t)-ERK1/2, p-p38/t-p38, and p-MAPK kinase 1 (MEK)/t-MEK in the miR-4500 mimic group decreased significantly (all $p < 0.05$), and the MAPK signaling pathway was inhibited. Compared with the si-

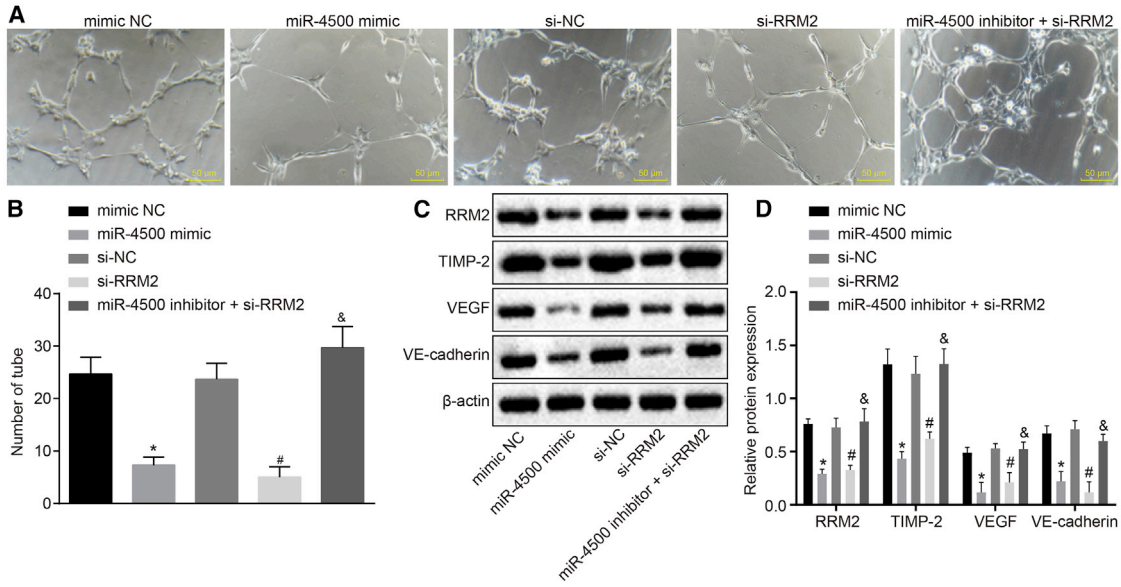


**Figure 7. Overexpression of miR-4500 Downregulates RRM2 to Inhibit the Capillary-Like Tube Formation of Endothelial Cells and the Angiogenesis of Breast Cancer Cells**

(A) Capillary-like tube formation observed under a microscope by in vitro Matrigel-based tube formation assay (200 ×). (B) Comparison of the number of tube in each group. (C) The protein expressions of tumor angiogenic factors TIMP-2, VEGF and VE-cadherin detected by Western blot. (D) Comparison of relative protein expressions of tumor angiogenic factors TIMP-2, VEGF and VE-cadherin in each group. *, #, and &$p < 0.05$ versus the mimic NC group, si-NC group, and si-RRM2 group, respectively. The data comparisons were analyzed by one-way ANOVA, and the experiment was repeated three times independently.

NC group, the expressions of p-ERK/t-ERK, p-p38/t-p38, and p-MEK/t-MEK were all decreased in the si-RRM2 group (all $p < 0.05$). Meanwhile, the expressions of p-ERK/t-ERK, p-p38/t-p38, and p-MEK/t-MEK in the miR-4500 inhibitor + si-RRM2 group were all significantly elevated compared to the si-RRM2 group (all $p < 0.05$), which illustrated that miR-4500 downregulated RRM2 to inhibit the activation of the MAPK signaling pathway.

### Overexpression of miR-4500 Inhibits Tumor Growth of Breast Cancer *In Vivo* through Downregulation of RRM2

The tumor xenograft was induced in nude mice to detect the influence of miR-500 overexpression on the tumor volume and size of breast cancer (Figures 9A and 9B). No significant changes were detected in tumor volume between the mimic NC group and the si-NC group after 14 days of growth ($p > 0.05$). Compared with the mimic NC group, the tumor growth rate and tumor volume of the nude mice were reduced in the miR-4500 mimic group ($p < 0.05$). Meanwhile, the tumor growth rate and tumor volume of nude mice were decreased in the si-RRM2 group compared to the si-NC group ($p < 0.05$). Relative to the si-RRM2 group, the tumor growth rate of nude mice was accelerated, and the tumor volume was increased in the miR-4500 inhibitor + si-RRM2 group ($p < 0.05$). These results demonstrated that miR-4500 downregulated RRM2 to inhibit tumor growth of breast cancer *in vivo*.

## DISCUSSION

More and more studies have highlighted the important role of miRNA expressions in the progression of breast cancer, with prospective use in tumor classification and prognosis prediction.[17] However, very few studies have investigated the role of miR-4500 functioning in breast cancer. Tackling this head on, the current study aimed to elucidate the role of miR-4500 in breast cancer and uncovered that miR-4500 inactivates the MAPK signaling pathway through downregulation of RRM2, thus restricting the development of breast cancer.

Initially, our results illustrated that miR-4500 is poorly expressed in breast cancer cell lines, and RRM2 was a target gene of miR-4500. Similarly, another study documented low expression of miR-4500 in NSCLC cells, and downregulation of miR-4500 promoted tumor growth by targeting LIN28B and NRAS in NSCLC.[7] Besides, Yu et al.[8] also revealed that miR-4500 was expressed poorly in CRC cells and further indicated that miR-4500 serves as a novel tumor suppressor by regulating HMGA2. Our findings also demonstrated that overexpression of miR-4500 downregulated the RRM2 gene and further inhibited the activation of the MAPK signaling pathway. This is noteworthy, as another miRNA, miR-433, is known to play a critical role in suppressing breast cancer cell proliferation, migration, and invasion through inhibition of the MAPK signaling pathway.[18] In addition, Mutlu et al.[19] proposed that miR-564 directly targeted a network of genes and regulated both phosphatidylinositol 3-kinase (PI3K) and the MAPK signaling pathway to influence breast cancer cell proliferation, migration, and invasion, which is in line with our results. Based on the information above, we predict that miR-4500 is poorly expressed in breast cancer cells, and overexpression of miR-4500 inhibits the MAPK signaling pathway through negative regulation of RRM2.

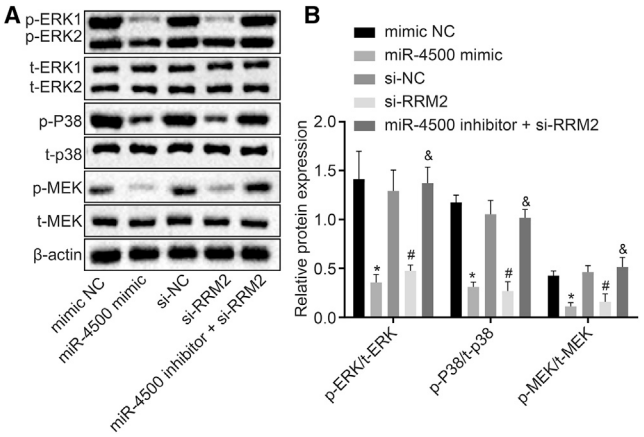


**Figure 8. Overexpression of miR-4500 Inhibits the Expression of RRM2 to Inhibit Activation of the MAPK Signaling Pathway**

(A) The protein expressions of p-ERK/t-ERK, p-p38/t-p38 and p-MEK/t-MEK detected by Western blot. (B) Comparison of relative protein expression of p-ERK/t-ERK, p-p38/t-p38, and p-MEK/t-MEK in each group. *, #, and &p < 0.05 versus the mimic NC group, si-NC group, and si-RRM2 group, respectively. The data comparisons were analyzed by one-way ANOVA, and the experiment was repeated three times independently.

In the subsequent assays, we discovered that overexpression of miR-4500 downregulated RRM2, which consequently inhibited proliferation, migration, invasion, and angiogenesis of breast cancer cells while promoting apoptosis. Moreover, overexpressed miR-4500 brought about a decline in the expressions of migration- and invasion-related factors MMP-2 and MMP-9; proliferation-related factors Ki67 and PCNA; and tumor angiogenic factors TIMP-2, VEGF, and VE-cadherin; meanwhile, the expression levels of apoptosis-related factors c-caspase-3/t-caspase-3 and c-caspase-9/t-caspase-9 were significantly elevated. Likewise, miR-141 was downregulated in breast cancer, and overexpression of miR-141 was associated with clinicopathologic features, such as decreased expressions of proliferation-related factors Ki67, human epidermal growth factor receptor 2 (HER2), and PCNA.[20] Meanwhile, Ni et al.[21] revealed that miR-106b overexpression accounts for one of the mechanisms underlying downregulation of the migration- and invasion-related factor MMP-2 and in turn, inhibits breast cancer metastasis and invasion. In addition, Chen et al.[22] demonstrated that overexpression of miR-4443 led to obvious reductions in the expressions of the tumor angiogenic factor, TIMP-2, and further suppressed tumor angiogenesis in breast cancer cells. Another possible explanation was that the level of caspase-3 increased obviously after miR-490-5p overexpression, in contrast to the controls, which suggested that miR-490-5p could promote bladder cancer cell line T24 cell apoptosis.[23] Furthermore, results obtained from the *in vivo* assay of our study verified and illustrated that overexpression of miR-4500 downregulated RRM2 and further inhibited tumor growth of breast cancer.

In conclusion, findings from the current study highlighted miR-4500 as a novel tumor suppressor in breast cancer. With our *in vitro* and *in vivo* assays, we demonstrated that miR-4500-mediated RRM2 downregulation inhibits proliferation, angiogenesis, invasion, and migration of breast cancer cells and promotes apoptosis through inhibition of MAPK signaling pathway activation (Figure 10). Thus, we feel, based on the evidence of this study, that therapeutic strategies should be directed toward the upregulation of miR-4500 in the future, which may potentially be a clinically viable target in the treatment of breast cancer. Further studies on clinical tissues from patients and more breast cancer cell lines are required to fully understand the detailed mechanisms of miR-4500 in breast cancer.

## MATERIALS AND METHODS

### Ethics Statement

All animal experimental protocols were approved by the Ethnic Committee of Jinan University-Affiliated Shenzhen Baoan Women's and Children's Hospital and conducted in strict accordance with the standard of the Guide for the Care and Use of Laboratory Animals published by the Ministry of Science and Technology of the People's Republic of China. Great efforts were made to minimize the number and suffering of the included animals.

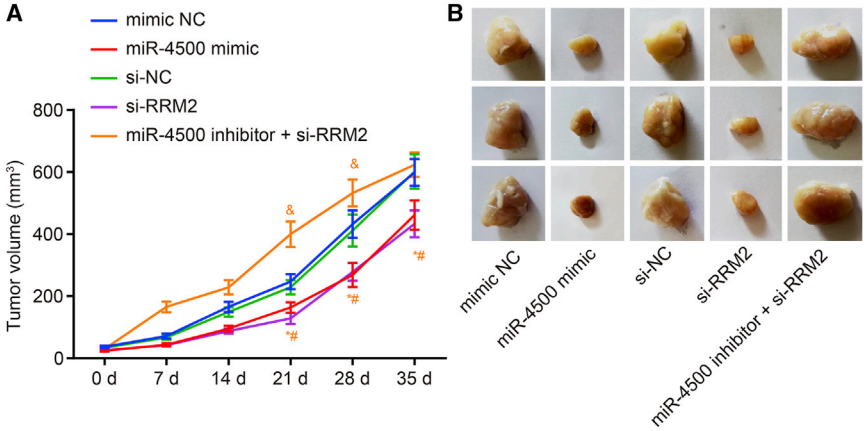


**Figure 9. Overexpression of miR-4500 Downregulates RRM2 to Inhibit Breast Cancer Growth *In Vivo***

(A) The growth of tumor volume in nude mice of each group after transfection and inoculation. (B) The tumor volume *in vivo* in each group detected by nude mice tumor xenograft assay. *, #, and &p < 0.05 versus the mimic NC group, si-NC group, and si-RRM2 group, respectively. The experiment was repeated three times independently, and data comparison at different time points in the figure was analyzed with repeated-measures ANOVA.

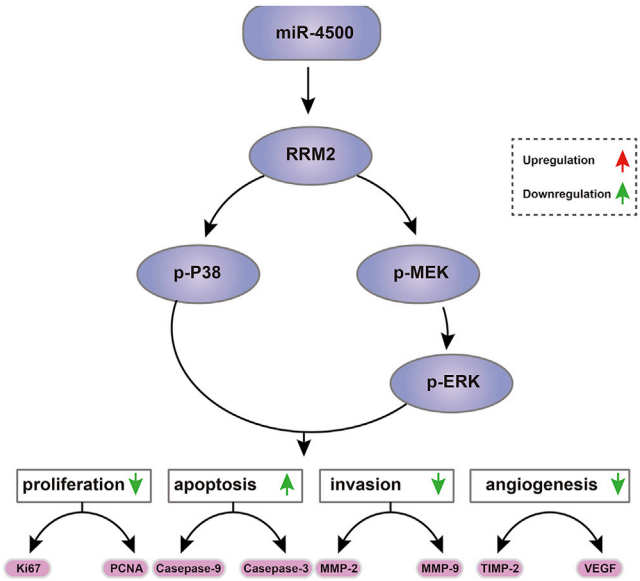


**Figure 10. The Mechanism of miR-4500 in Breast Cancer Cells with the Involvement of RRM2 and the MAPK Signaling Pathway**

Overexpression of miR-4500 downregulates RRM2 to inhibit the activation of the MAPK signaling pathway, thus inhibiting proliferation, invasion, migration, and tumor angiogenesis and promoting apoptosis of breast cancer cells.

### Microarray-Based Gene-Expression Analysis

First, breast cancer-related microarrays were retrieved from the GEO database (https://www.ncbi.nlm.nih.gov/geo/). The "limma" package of R language was applied to perform variance analysis on gene expression in the microarray. |logFoldChange| >2 and p <0.05 were regarded as the criteria for screening the DEGs. A heatmap of the obtained DEGs was constructed using the "pheatmap" package.

### KEGG Analysis

ClueGO, a Cytoscape plug-in, is capable of creating and visualizing a functionally grouped network of terms/pathways for large clusters of genes, which can be uploaded from a text file or interactively from the Cytoscape network. KEGG analysis of the obtained DEGs was carried out with help of this software.

### Gene-Interaction Analysis

Known breast cancer-related genes were retrieved from the MalaCards database (https://www.malacards.org/), and the top ten genes with high scores were selected for subsequent analysis. Subsequently, association analysis of the retrieved genes and the DEGs was performed using the Search Tool for the Retrieval of Interacting Genes/Proteins database (https://string-db.org/). The interaction network diagram of DEGs was constructed with the Cytoscape software.

### miRNA Prediction

miRNAs, which regulated RRM2, were predicted by the DIANA database (http://diana.imis.athena-innovation.gr/DianaTools/index.php?r=microT_CDS/index), miRDB database (http://mirdb.org/miRDB/index.html), miRSearch database (https://www.exiqon.com/miRSearch), and microRNA Data Integration Portal (mirDIP) database (http://ophid.utoronto.ca/mirDIP/index.jsp#r), and the miRNA in the intersection of the predicted results was selected.

### Cell Line Screening

Breast cancer cell lines, including MCF7, BT474, MDA-MB-468, MDA-MB-231, and normal human mammary epithelial cell line MCF10A, were obtained from the American Type Culture Collection (ATCC; Manassas, VA, USA). Each cell line was cultured in high-glucose Dulbecco's modified eagle medium (DMEM; Gibco, Grand Island, NY, USA) with 10% fetal bovine serum (FBS; Hangzhou Sijiqing Bioengineering Material, Hangzhou, Zhejiang, China) and 1% penicillin-streptomycin (100 U/L penicillin and 100 U/L streptomycin; Gibco, NY, USA) and placed in a saturated humidity atmosphere containing 5% $CO_2$ in air at 37°C. The culture medium was replaced every 2 or 3 days, and cells at the logarithmic phase of growth were selected for further experimentation. qRT-PCR was adopted to detect the expression of miR-4500 in different breast cancer cell lines.

### Cell Culture, Grouping, and Transfection

Cells were treated with 0.25% trypsin for subculture in DMEM containing 10% FBS at the ratio of 1:2. Next, the cells were incubated in a 5% $CO_2$ incubator at 37°C after adding the medium. The cells were passaged after fusion every 3 days and treated with 0.25% trypsin for 30 s to collect the medium containing cells. Then, the medium was centrifuged for 2 min at 179 × *g* with the supernatant removed. After that, the cells were resuspended with DMEM containing 10% FBS and penicillin/streptomycin (1 mL) at room temperature. The cells were then assigned into two aseptic culture flasks at the ratio of 1:2 to 1:5, and the complete medium was supplemented to 4 mL. The cells were cultured in 5% $CO_2$ at 37°C, and cells at the logarithmic phase of growth were chosen for the subsequent experiments. Breast cancer cells were allocated into the following 8 groups: miR-4500 mimic group, mimic NC group, miR-4500 inhibitor group, inhibitor NC group, si-RRM2 group, si-NC group, miR-4500 inhibitor + si-RRM2 group, and miR-4500 mimic + si-RRM2 group. The cells were seeded into a 6-well plate for 24 h prior to transfection. When cell confluence reached about 50%, the human breast cancer cells were transiently transfected with the mediation of Lipofectamine 2000 (Invitrogen, Carlsbad, CA, USA). The medium was replaced after 6 h of transfection, and the cells were collected after 48 h of culture for subsequent experimentation.

### Dual-Luciferase Reporter Gene Assay

The target gene of miR-4500 was predicted by the biological prediction website http://www.microrna.org/microrna/home.do. Subsequently, the binding relationship between miR-4500 and RRM2 and whether RRM2 was a direct target gene of miR-4500 were verified. The synthetic miRNA (RRM2) 3′ UTR gene fragment was introduced into pMIR-REPORT (Beijing Huayueyang Biotechnology, Beijing, China) by SpeI and HindIII restriction endonuclease cleavage sites. The complementary sequence mutation site of the seed sequence in the miRNA (RRM2) WT was designed. The target

**Table 2. Primer Sequence of qRT-PCR**

| Gene | Primer Sequence |
|---|---|
| miR-4500 | F: 5′-UGAGGUAGUAGUUUCUUTAA-3′ |
| | R: 5′-GCATCAATGGACAACA-3′ |
| RRM2 | F: 5′-CTATGGTGAACGTGTTGATAGCCTT-3′ |
| | R: 5′-GTCCTCGTTTCTTGAGCCAGA-3′ |
| U6 | F: 5′-CGCTTCGGCAGCACATATACTA-3′ |
| | R: 5′-CGCTTCACGAATTTGCGTGTCA-3′ |
| GAPDH | F: 5′-ACAACAGCCTCAAGATCATCAG-3′ |
| | R: 5′-GGTCCACCACTGACACGTTG-3′ |

F, forward; R, reverse.

fragment was inserted into the pMIR-REPORT plasmid with T4 DNA ligase through restriction endonuclease digestion. Next, the correctly sequenced luciferase reporter plasmids WT and MUT were cotransfected, respectively, with miR-4500 mimic into HEK293T cells (Shanghai Beinuo Biotechnology, Shanghai, China). Cells were then collected and lysed after 48 h of transfection, and the luciferase activity was detected with a luciferase assay kit (K801-200; BioVisionTechnologies, San Francisco, CA, USA) and GloMax 20/20 luminometer (Promega, Madison, WI, USA).

### qRT-PCR

RNA extraction kits (Invitrogen, Carlsbad, CA, USA) were employed to extract the total RNA content of breast cancer cell lines from each group. Primers were synthesized by Takara Biotechnology (Dalian, Liaoning, China) (Table 2). After extraction, the RNA was reverse transcribed into cDNA, according to the instructions of the PrimeScript RT kit. Reaction solution was taken for fluorescence qPCR, according to the instructions of the SYBR Premix Ex Taq II kit. The fluorescence qPCR was carried out in the ABI PRISM 7300 system. U6 was regarded as the internal reference of the relative expression levels of miR-4500, and glyceraldehyde-3-phosphate dehydrogenase (GAPDH) was the internal reference of the relative expression levels of RRM2. The relative transcription levels of the target genes were calculated using the $2^{-}\Delta^{Ct}$ method, and the relative mRNA levels of target gene were $2^{-\Delta\Delta Ct}$.[24]

### Western Blot Analysis

Total protein content was extracted, and the protein concentration was determined with bicinchoninic acid kits (Thermo Fisher Scientific, Waltham, MA, USA). With the use of sodium dodecyl sulfate polyacrylamide gel electrophoresis, the total proteins (30 μg) were electrophoresed at a stable voltage of 80 V for 35 min and then changed to 120 V for 45 min. After that, the proteins were transferred onto a polyvinylidene fluoride membrane (Amersham, GE Healthcare, Chicago, IL, USA). Next, the membrane was blocked with 5% skimmed milk at room temperature for 1 h and incubated at 4°C with the primary antibody rabbit polyclonal antibody to RRM2 (dilution ratio of 1:5,000, ab172476), ERK1/ERK2 (dilution ratio of 1:10,000, ab184699), p38 (dilution ratio of 1:1,000, ab31828), MEK1 (dilution ratio of 1:1,000, ab96379), Ki67 (dilution ratio of 1:5,000, ab209897), PCNA (dilution ratio of 1:1,000, ab92552), MMP-2 (dilution ratio of 1:1,000, ab37150), MMP-9 (dilution ratio of 1:1,000, ab73734), TIMP-2 (dilution ratio of 1:1,000, ab1828), VEGF (dilution ratio of 1:1,000, ab32152), and β-actin (dilution ratio of 1:5,000, ab8227). All of the primary antibodies were purchased from Abcam (Cambridge, UK). The membrane was rinsed with phosphate-buffered saline (PBS) containing 0.1% Tween-20 (PBST), 3 times, 15 min each, and incubated with the goat anti-rabbit secondary antibody labeled with horseradish peroxidase (dilution ratio of 1:10,000; Jackson ImmunoResearch Laboratories, Westgrove, PA, USA) at room temperature for 1 h. The membrane was then washed with PBST, 3 times, 10 min each. Immunoreactive proteins were visualized by enhanced chemiluminesecence. ImageJ software was employed to analyze the gray value of the target band.

### EdU Proliferation Assay

The breast cancer cell lines at the logarithmic growth phase were selected and seeded in a 96-well plate (density of $2 \times 10^3$ to $4 \times 10^4$ cells/well) and cultured to a normal growth stage. The cells adhering to the walls after 24 h were transfected with 3 parallel wells per group. Meanwhile, cells that were transfected for 48 h were labeled with EdU. The cells were then incubated with EdU medium (100 μL/well) for 2 h, rinsed twice with PBS, added with cell fixative (100 μL/well), and incubated at room temperature for 30 min. Next, the cells were incubated with 2 mg/mL glycine for 5 min, rinsed with PBS (100 μL/well) for 5 min, incubated with 100 μL/well penetrant (PBS containing 0.5% Triton X-100) for 10 min, and rinsed with PBS. Afterward, the cells were supplemented with 1 × Apollo staining reaction solution; incubated, devoid of light for 30 min; added with penetrant; and washed with methanol. Subsequently, the cells were added with 1 × 4′,6-diamidino-2-phenylindole (DAPI) reaction solution (100 μL/well); incubated, devoid of light at room temperature; decolorized; shaken; incubated for 30 min; and then washed with PBS (100 μL/well) three times. Finally, the cells were added with anti-fluorescence-quenching tablets (100 μL/well). A random selection of 6–10 fields per well was observed with a fluorescence microscope and photographed.

### Hoechst Staining

The breast cancer cells at the logarithmic growth phase were detached with 0.25% trypsin and seeded in 6-well plates (density of 1 × 10 cells/well). Subsequently, the cells were treated with different concentrations of drugs for 48 h, and the culture medium was removed. The cell precipitates were suspended and fixed in 300 μL formaldehyde (4%) for 30 min, rinsed with PBS, and centrifuged to collect cells. The cells were then stained with 100 μL Hoechst-33342 (Sigma-Aldrich, St. Louis, MO, USA) for 10 min. Finally, the suspension was dripped onto the slide covered with glass, observed, and photographed under a fluorescent microscope.

### Transwell Migration and Invasion Assays

The Transwell chamber with 0.8 μm aperture (Corning Glass Works, Corning, NY, USA) was employed for migration assay, and Transwell

with 0.8 μm aperture (Becton Dickinson, Franklin Lakes, NJ, USA) was applied for invasion assay. The cells at passage 3 were allowed to reach 80% confluence and starved for 24 h, and serum-free DMEM was then added to the basolateral chamber (Corning Glass Works, Corning, NY, USA) and placed at 37°C for 1 h. The cells were then resuspended in serum-free DMEM after detachment, counted, and diluted to $3 \times 10^5$ cells/mL. The apical chamber was added with 100 μL cells; meanwhile, the basolateral chamber was added with 600 μL DMEM containing 10% serum (the serum was considered as chemokine). The cells were cultured for 24 h, according to the instructions of the Transwell chamber, and then the cells of apical chamber were cleaned. After that, the chamber was rinsed with PBS and immersed with precooled methanol for 30 min. Cells transferred to the basolateral chamber were fixed and stained with 0.1% crystal violet for 10 min. Six visual fields were selected, and the cells were observed, photographed, and counted under an inverted microscope (Olympus Optical, Tokyo, Japan). A cell-invasion assay was carried out using Matrigel. The Matrigel stored in the refrigerator at −20°C was melted at 4°C and then diluted with serum-free DMEM at a ratio of 1:10. The concentration of seeded cells was adjusted to $1.0 \times 10^5$ cells/mL. Other operations were the same as the cell-migration procedures. The numbers of cell migration and invasion were counted.

### Matrigel-Based Capillary-Like Tube-Formation Assay

Matrigel (356234; Shanghai Shanran Biotechnology, Shanghai, China) was placed at 4°C overnight to melt into a yellow gelatinous liquid, and 70 μL of the Matrigel (with a thickness of 0.5 mM) was added to the precooled 96-well plates using precooled Finnpipette. The cell-culture plate was positioned in an incubator for about 30 min at 37°C and concreted. The human umbilical vein endothelial cells (HUVECs) at the logarithmic growth phase were seeded with 50 μL cell suspension with 5,000 cells/well, and 50 μL of supernatants of breast cancer cells transfected with different plasmids was added to the well, respectively. HUVECs were cultured for 24 h at 37°C and observed under a Leica inverted-phase contrast microscope. The number of capillary-like structures was calculated using the Image-Pro Plus software (version 6.0) under a microscope.

### Tumor Xenograft in Nude Mice

Forty male-specific pathogen-free-grade nude mice (aged 5 weeks, weighing 15–22 g) were purchased from Shanghai SLAC Laboratory Animal (Shanghai, China). The nude mice were raised under conditions of stable temperature (25°C–27°C) and humidity (45%–50%). Next, the mice were randomly assigned into the following 5 groups (n = 8): mimic NC group, miR-4500 mimic group, si-NC group, si-RRM2 group, and miR-4500 inhibitor + oe-RRM2 group. Mice were then inoculated with the cell suspension after adequate anesthesia. The stably transfected cells at the logarithmic growth phase were resuspended in 50% Matrigel (Becton Dickinson, Franklin Lakes, NJ, USA), and the cell concentration was adjusted to $2 \times 10^6$ cells/mL. Then, 0.2 mL single-cell suspension (containing $4 \times 10^5$ cells) was subcutaneously injected into the left axillary of each mouse. The mice were observed for 3 weeks until the presence of tumor. After that, the tumor was excised from the nude mice and measured for weight and volume, and the hemoglobin content was also calculated. Some of the tumors were frozen in a liquid nitrogen tube, whereas others were placed in Bowen's fixed solution for immunohistochemistry.

### Statistical Analysis

Statistical analyses were conducted using SPSS 21.0 software (IBM, Armonk, NY, USA). Measurement data were expressed as mean ± standard deviation. Comparisons between two groups were conducted by the unpaired t test. Data of multiple groups were compared by one-way analysis of variance (ANOVA) and post-test test. Data comparisons at different time points were analyzed with repeated-measures ANOVA. The rank-sum test was applied to analyze skewed distribution data. A value of $p < 0.05$ indicated statistical significance.

## SUPPLEMENTAL INFORMATION

Supplemental Information can be found online at https://doi.org/10.1016/j.omtn.2020.04.018.

## AUTHOR CONTRIBUTIONS

S.L., H.M., and Y.Z. designed the study. G.L., J.S., G.L., B.L., and S.C. collated the data, designed and developed the database, carried out data analyses, and produced the initial draft of the manuscript. S.L. contributed to drafting the manuscript. All authors have read and approved the final submitted manuscript.

## CONFLICTS OF INTEREST

The authors declare no competing interests.

## ACKNOWLEDGMENTS

This study was supported by the Project of the Department of Science and Technology of Guangdong Province (2015A020211003), Shenzhen Science and Technology Innovation Committee (JCYJ20150403105513703), Sanming Project of Medicine in Shenzhen (SZSM201406007) and the Project of Shenzhen Science and Technology Innovation Comittee entitled."The Study Mechanisms of LncRNA PVT1 in the Development of Breast Cancer through Promoting Methylation of LAMA2 Promoter".

## REFERENCES

1. Wong, I.O., Scholing, C.M., Cowling, B.J., and Leung, G.M. (2015). Breast cancer incidence and mortality in a transitioning Chinese population: current and future trends. Br. J. Cancer *112*, 167–170.
2. He, D., Fang, Y., Gunter, M.J., Xu, D., Zhao, Y., Zhou, J., Fang, H., and Xu, W.H. (2017). Incidence of breast cancer in Chinese women exposed to the 1959-1961 great Chinese famine. BMC Cancer *17*, 824.
3. Thomson, A.K., Heyworth, J.S., Girschik, J., Slevin, T., Saunders, C., and Fritschi, L. (2014). Beliefs and perceptions about the causes of breast cancer: a case-control study. BMC Res. Notes *7*, 558.
4. Zhou, S., Li, J., Xu, H., Zhang, S., Chen, X., Chen, W., Yang, S., Zhong, S., Zhao, J., and Tang, J. (2017). Liposomal curcumin alters chemosensitivity of breast cancer cells to Adriamycin via regulating microRNA expression. Gene *622*, 1–12.
5. Duan, Z., Choy, E., Harmon, D., Liu, X., Susa, M., Mankin, H., and Hornicek, F. (2011). MicroRNA-199a-3p is downregulated in human osteosarcoma and regulates cell proliferation and migration. Mol. Cancer Ther. *10*, 1337–1345.

6. Farhana, L., Dawson, M.I., and Fontana, J.A. (2015). Down regulation of miR-202 modulates Mxd1 and Sin3A repressor complexes to induce apoptosis of pancreatic cancer cells. Cancer Biol. Ther. *16*, 115–124.

7. Zhang, L., Qian, J., Qiang, Y., Huang, H., Wang, C., Li, D., and Xu, B. (2014). Down-regulation of miR-4500 promoted non-small cell lung cancer growth. Cell. Physiol. Biochem. *34*, 1166–1174.

8. Yu, F.Y., Tu, Y., Deng, Y., Guo, C., Ning, J., Zhu, Y., Lv, X., and Ye, H. (2016). MiR-4500 is epigenetically downregulated in colorectal cancer and functions as a novel tumor suppressor by regulating HMGA2. Cancer Biol. Ther. *17*, 1149–1157.

9. Zhao, H., Zhang, H., Du, Y., and Gu, X. (2014). Prognostic significance of BRCA1, ERCC1, RRM1, and RRM2 in patients with advanced non-small cell lung cancer receiving chemotherapy. Tumour Biol. *35*, 12679–12688.

10. Sukhtankar, D., Okun, A., Chandramouli, A., Nelson, M.A., Vanderah, T.W., Cress, A.E., Porreca, F., and King, T. (2011). Inhibition of p38-MAPK signaling pathway attenuates breast cancer induced bone pain and disease progression in a murine model of cancer-induced bone pain. Mol. Pain *7*, 81.

11. Kobayashi, A., Kanaba, T., Satoh, R., Ito, Y., Sugiura, R., and Mishima, M. (2017). Chemical shift assignments of the first and second RRMs of Nrd1, a fission yeast MAPK-target RNA binding protein. Biomol. NMR Assign. *11*, 123–126.

12. Haque, I.U. (1979). Tibio-fibular synostosis for the treatment of tibial defects. Med. J. Zambia *13*, 91–93.

13. Deng, Z.Q., Yin, J.Y., Tang, Q., Liu, F.Q., Qian, J., Lin, J., Shao, R., Zhang, M., and He, L. (2014). Over-expression of miR-98 in FFPE tissues might serve as a valuable source for biomarker discovery in breast cancer patients. Int. J. Clin. Exp. Pathol. *7*, 1166–1171.

14. Siragam, V., Rutnam, Z.J., Yang, W., Fang, L., Luo, L., Yang, X., Li, M., Deng, Z., Qian, J., Peng, C., and Yang, B.B. (2012). MicroRNA miR-98 inhibits tumor angiogenesis and invasion by targeting activin receptor-like kinase-4 and matrix metalloproteinase-11. Oncotarget *3*, 1370–1385.

15. Wang, Y., Bao, W., Liu, Y., Wang, S., Xu, S., Li, X., Li, Y., and Wu, S. (2018). miR-98-5p contributes to cisplatin resistance in epithelial ovarian cancer by suppressing miR-152 biogenesis via targeting Dicer1. Cell Death Dis. *9*, 447.

16. Wang, L., Guo, S., and Zhang, H. (2017). MiR-98 Promotes Apoptosis of Glioma Cells via Suppressing IKBKE/NF-κB Pathway. Technol. Cancer Res. Treat. *16*, 1226–1234.

17. Fu, S.W., Chen, L., and Man, Y.G. (2011). miRNA Biomarkers in Breast Cancer Detection and Management. J. Cancer *2*, 116–122.

18. Zhang, T., Jiang, K., Zhu, X., Zhao, G., Wu, H., Deng, G., and Qiu, C. (2018). miR-433 inhibits breast cancer cell growth via the MAPK signaling pathway by targeting Rap1a. Int. J. Biol. Sci. *14*, 622–632.

19. Mutlu, M., Saatci, Ö., Ansari, S.A., Yurdusev, E., Shehwana, H., Konu, Ö., Raza, U., and Şahin, Ö. (2016). miR-564 acts as a dual inhibitor of PI3K and MAPK signaling networks and inhibits proliferation and invasion in breast cancer. Sci. Rep. *6*, 32541.

20. Li, P., Xu, T., Zhou, X., Liao, L., Pang, G., Luo, W., Han, L., Zhang, J., Luo, X., Xie, X., and Zhu, K. (2017). Downregulation of miRNA-141 in breast cancer cells is associated with cell migration and invasion: involvement of ANP32E targeting. Cancer Med. *6*, 662–672.

21. Ni, X., Xia, T., Zhao, Y., Zhou, W., Wu, N., Liu, X., Ding, Q., Zha, X., Sha, J., and Wang, S. (2014). Downregulation of miR-106b induced breast cancer cell invasion and motility in association with overexpression of matrix metalloproteinase 2. Cancer Sci. *105*, 18–25.

22. Chen, X., Zhong, S.L., Lu, P., Wang, D.D., Zhou, S.Y., Yang, S.J., Shen, H.Y., Zhang, L., Zhang, X.H., Zhao, J.H., and Tang, J.H. (2016). miR-4443 Participates in the Malignancy of Breast Cancer. PLoS ONE *11*, e0160780.

23. Lan, G., Yang, L., Xie, X., Peng, L., and Wang, Y. (2015). MicroRNA-490-5p is a novel tumor suppressor targeting c-FOS in human bladder cancer. Arch. Med. Sci. *11*, 561–569.

24. Ayuk, S.M., Abrahamse, H., and Houreld, N.N. (2016). The role of photobiomodulation on gene expression of cell adhesion molecules in diabetic wounded fibroblasts in vitro. J. Photochem. Photobiol. B *161*, 368–374.

**OMTN, Volume *21***

## Supplemental Information

# MicroRNA-4500 Inhibits Migration, Invasion, and Angiogenesis of Breast Cancer Cells via RRM2-Dependent MAPK Signaling Pathway

**Shaoying Li, Huifen Mai, Yefeng Zhu, Guofeng Li, Jing Sun, Guisen Li, Bichan Liang, and Shaojun Chen**

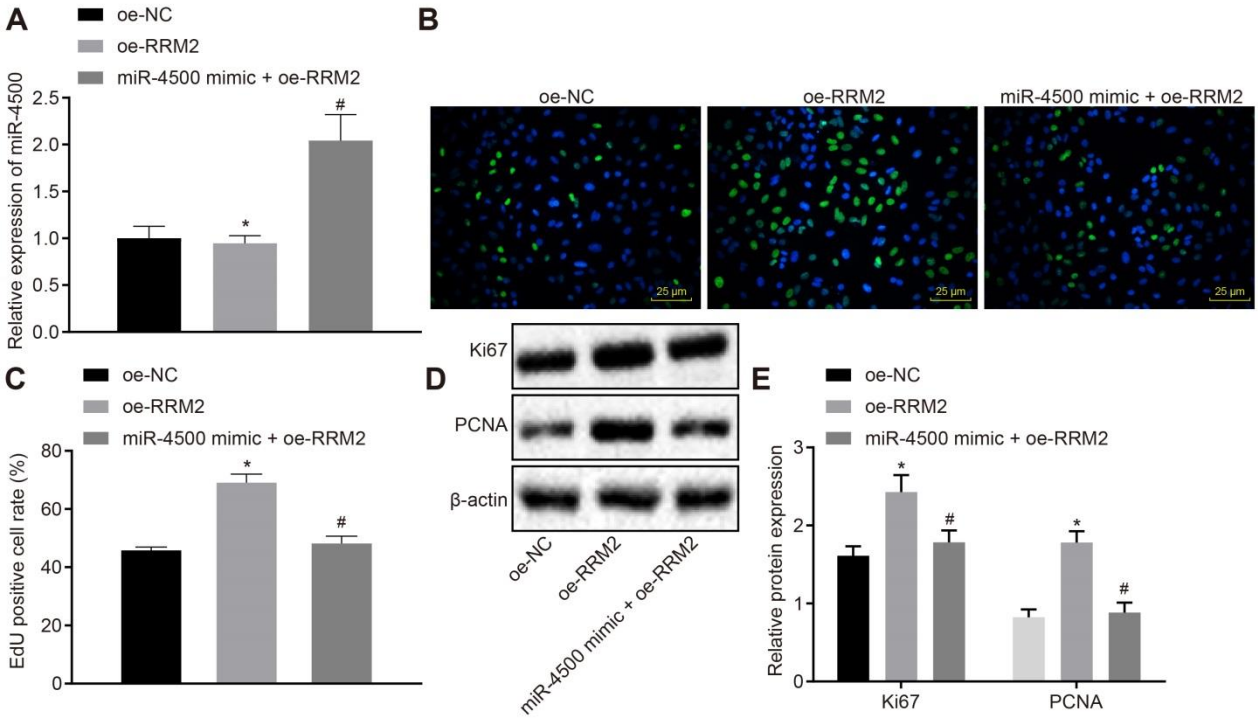


**Supplementary Figure 1. Over-expressed RRM2 promotes proliferation of breast cancer cells, which is abrogated by up-regulated miR-4500.**

A, The expression patterns of miR-4500 determined by RT-qPCR. B, The cell proliferation detected by EdU proliferation assay (400 ×). C, The quantitative analysis for EdU positive breast cancer cells detected by EdU proliferation assay. D, The protein bands of RRM2 and cell proliferation-related factors Ki67 and PCNA in each group detected by Western blot analysis. D, The RRM2 and cell proliferation-related factors Ki67 and PCNA protein expression patterns in each group detected by Western blot analysis. *, # respectively indicate that $p < 0.05$ *vs.* the oe-NC group and oe-RRM2 group. The data comparisons were analyzed by one-way ANOVA and the experiment was repeated three times independently.

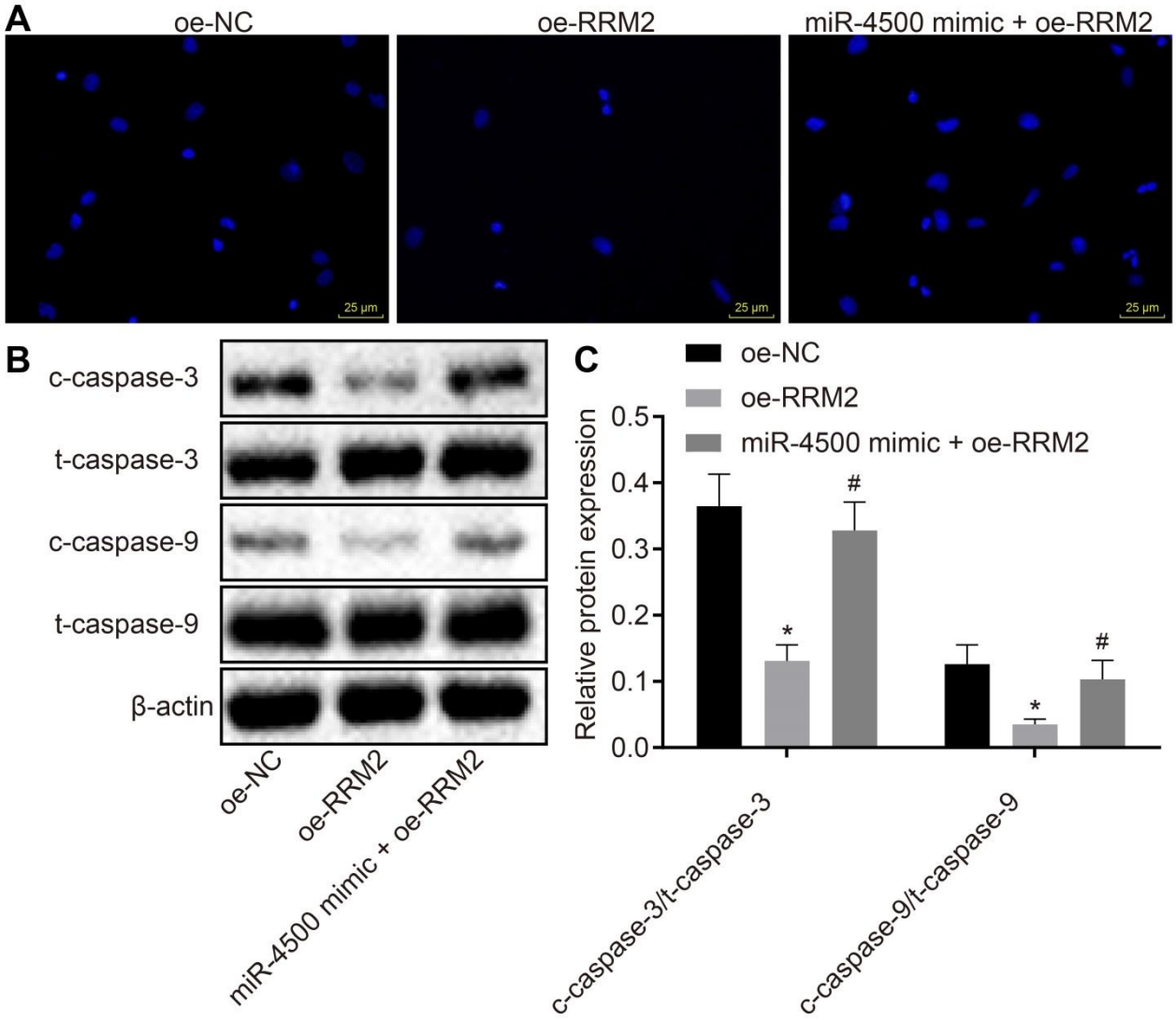


**Supplementary Figure 2. Over-expressed RRM2 inhibits apoptosis of breast cancer cells, which is abrogated by up-regulated miR-4500.**

A, The cell apoptosis detected by Hoechst staining (400 ×). B, The protein bands of cell apoptosis-related factors c-Caspase-3/t-Caspase-3 and c-Caspase-9/t-Caspase-9 detected by Western blot analysis. C, The protein expression patterns of cell apoptosis-related factors c-Caspase-3/t-Caspase-3 and c-Caspase-9/t-Caspase-9 in each group detected by Western blot analysis; *, # respectively indicate that $p < 0.05$ *vs.* the oe-NC group and oe-RRM2 group. The data comparisons were analyzed by one-way ANOVA and the experiment was repeated three times independently.

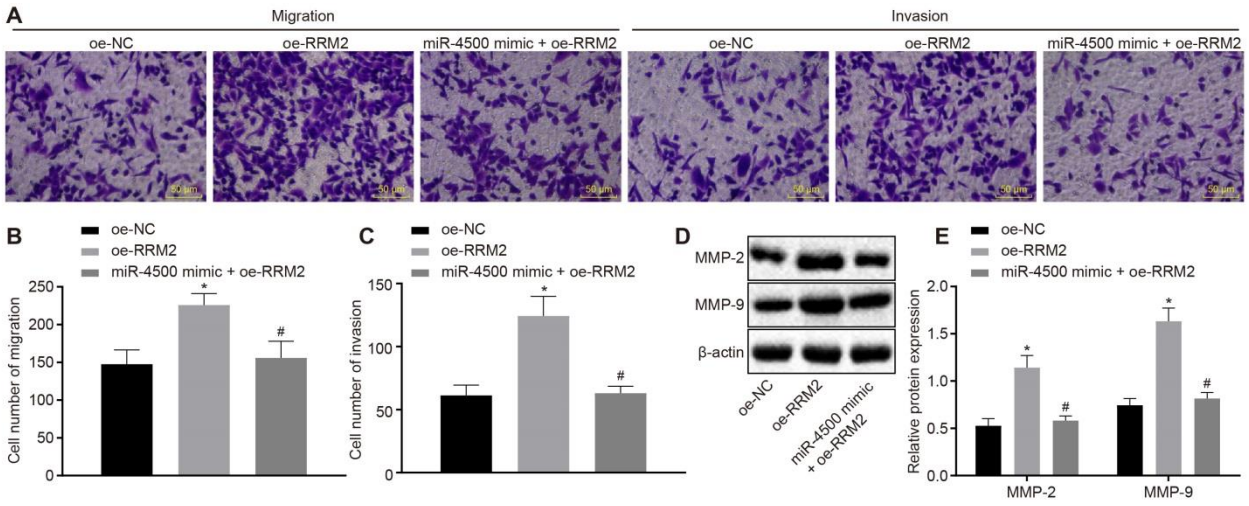


**Supplementary Figure 3. Over-expressed RRM2 promotes migration and invasion of breast cancer cells, which is abrogated by up-regulated miR-4500.**

A, The migration and invasion of breast cancer cells in each group under the microscope (200 ×). B, The cell migration in each group detected by Transwell assay. C, The cell invasion in each group detected by Transwell assay. D and E, The protein expression patterns of RRM2, MMP-2 and MMP-9 in each group detected by Western blot analysis. *, # respectively indicate that $p < 0.05$ *vs.* the oe-NC group and oe-RRM2 group. The data comparisons were analyzed by one-way ANOVA and the experiment was repeated three times independently.

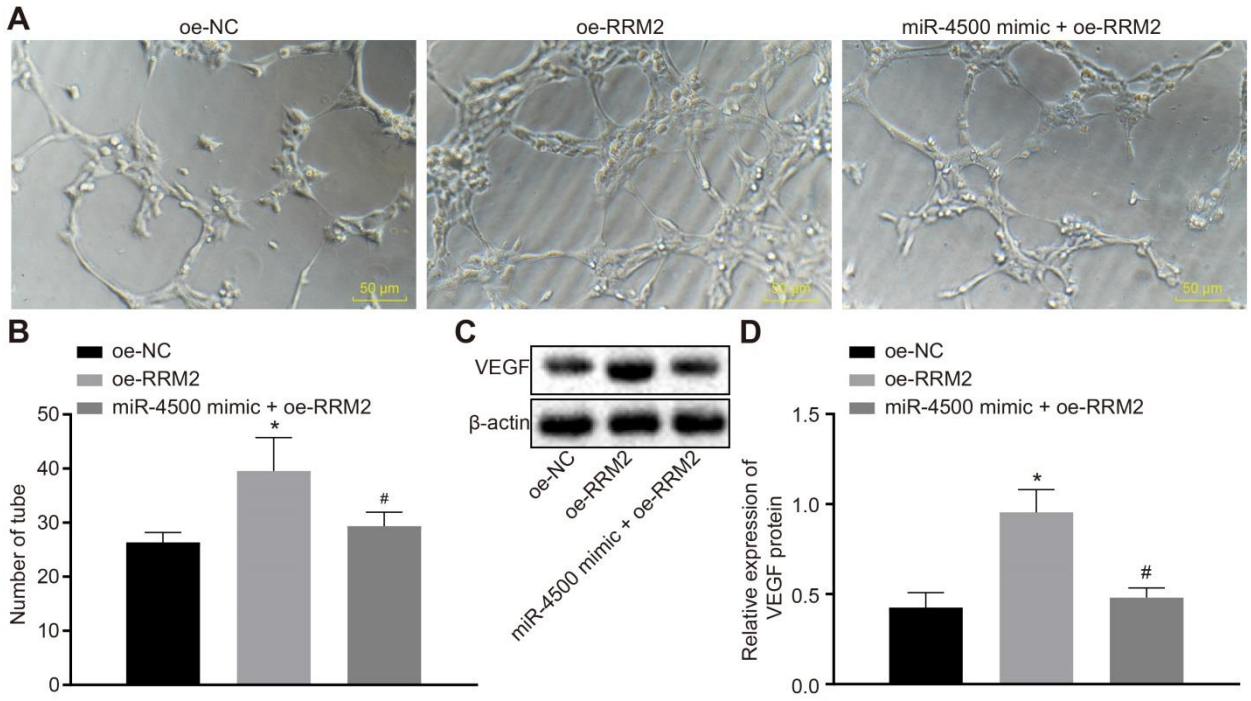


**Supplementary Figure 4. Over-expressed RRM2 promotes the capillary-like tube formation of endothelial cells and angiogenesis of breast cancer cells, which is abrogated by up-regulated miR-4500.**

A and B, Capillary-like tube formation observed under a microscope by *in vitro* assay (200 ×). C and D, The protein expressions of tumor angiogenic factor VEGF detected by Western blot analysis. *, # indicate that $p < 0.05$ respectively *vs.* the oe-NC group and oe-RRM2 group. The data comparisons were analyzed by one-way ANOVA and the experiment was repeated three times independently.